

# Electron capture by $\text{Ne}^{4+}$ ions from atomic hydrogen

C. C. Havener,\* R. Rejoub, C. R. Vane, and H. F. Krause  
*Physics Division, Oak Ridge National Laboratory, Oak Ridge, Tennessee 37831-6372, USA*

D. W. Savin and M. Schnell  
*Columbia Astrophysics Laboratory, Columbia University, New York, New York 10027-6601, USA*

J. G. Wang<sup>†</sup> and P. C. Stancil  
*Department of Physics and Astronomy and the Center for Simulational Physics, The University of Georgia, Athens, Georgia 30602-2451, USA*

(Received 24 June 2004; published 23 March 2005)

Using the Oak Ridge National Laboratory ion-atom merged-beams apparatus, the absolute total electron-capture cross section has been measured for collisions of  $\text{Ne}^{4+}$  with hydrogen and deuterium at relative energies in the center-of-mass frame between 0.10 and 1006 eV/u. Comparison with previous measurements shows large discrepancies between 80 and 600 eV/u. For energies below  $\sim 1$  eV/u, a sharply increasing cross section is attributed to the ion-induced dipole attraction between the reactants. Multichannel Landau-Zener calculations are performed between 0.01 and 5000 eV/u and compare well to the measured total cross sections. Below  $\sim 5$  eV/u, the present total cross section calculations show a significant target isotope effect. At 0.01 eV/u, the H:D total cross section ratio is predicted to be  $\sim 1.4$  where capture is dominated by transitions into the  $\text{Ne}^{3+}$  ( $2s^22p^23d$ ) configuration.

DOI: 10.1103/PhysRevA.71.034702

PACS number(s): 34.70.+e

## I. INTRODUCTION

Studies of electron-capture (EC) processes are motivated by the fact that they constitute reaction channels of fundamental importance in plasma environments. In astrophysics, EC by multicharged ions from H is important in planetary nebulae with hot central stars [1,2]. Accurate modeling of the Ne ion charge balance and radiative cooling in fusion energy plasmas requires reliable EC data for a wide range of energies and Ne ionization stages [3]. Systematic studies of the low-energy EC for  $\text{Ne}^{2+} + \text{H}$  and  $\text{Ne}^{3+} + \text{H}$  have recently been reported [4,5].

We are unaware of any published theoretical studies for low-energy EC in the  $\text{Ne}^{4+} + \text{H}$  collision system. Previous cross section measurements performed by Can *et al.* [6], Huber [7], and Seim *et al.* [8] at relatively high energies (i.e., above 60 eV/u) over a limited energy range indicate a decreasing cross section toward lower energies. At lower collision energies (eV/u), the ion-induced dipole interaction between reactants is important. The attractive force due to this potential and the resulting acceleration of the particles toward each other significantly modify the reactant trajectories. This results in the incident trajectories accessing internuclear distances smaller than the initial impact parameter. At low enough energies, these trajectory effects can dominate the electron transfer process and lead to enhanced cross sections [9]. Several systems have been investigated using the ORNL ion-atom merged-beams apparatus which show such enhancements [10]. Ion-induced dipole enhancements also lead to significant target isotope effects [11,12].

Here, using the ion-atom merged-beams apparatus, the absolute total cross section is measured for the electron transfer process



over four decades of collision energy, from 0.10 to 1006 eV/u. Below 250 eV/u, D is used instead of H. For comparison, multichannel Landau-Zener (MCLZ) calculations for collisions with H and D are performed over the energy range of 0.01 to 5000 eV/u. Due to the good agreement between the measured and calculated total cross sections, MCLZ calculations are also used to predict state-selective cross sections.

## II. EXPERIMENTAL APPROACH

In the merged-beam technique, relatively fast (keV) beams are collinearly merged producing a large dynamic range of relative collision energies in the center of mass (c.m.) [13]. In the present investigation, a  $^{20}\text{Ne}^{4+}$  beam with energies of 52–88 keV is merged with D beams at energies of 6.95–9.55 keV and a H beam at an energy of 6.70 keV, thereby allowing relative collision energies in the range of 0.10–1006 eV/u. The relative collision energy in the center-of-mass frame,  $E_{rel}$ , can be written in terms of the laboratory frame energies of the two beams  $E_1, E_2$  with masses  $m_1, m_2$ , as

$$E_{rel} \left( \frac{\text{eV}}{u} \right) = \frac{E_1}{m_1} + \frac{E_2}{m_2} - 2 \sqrt{\frac{E_1 E_2}{m_1 m_2}} \cos(\theta). \quad (2)$$

where  $u$  is the reduced mass,  $m_1 m_2 / (m_1 + m_2)$  and  $\theta$  is the merge angle between the two beams.

The ion-atom merged-beams apparatus has previously been described in detail [10,13]. A neutral ground state H

\*Electronic address: havenercc@ornl.gov

<sup>†</sup>Present address: Institute of Applied Physics and Computational Mathematics, P. O. Box 8009, Beijing 100089, P. R. China.

atom beam, obtained by photodetachment of a  $H^-$  beam, is nearly parallel (the divergence being less than  $0.15^\circ$ ) with a beam diameter of 2 mm and intensities ranging from 10 to 20 nA. Deuterium is used instead of hydrogen for c.m. energies below 250 eV/u to maximize the angular acceptance of the  $H^+$  ( $D^+$ ) detector [13,14].

The  $^{20}\text{Ne}^{4+}$  beam is produced by the ORNL CAPRICE ECR ion source [15] with an intensity of approximately  $4 \mu\text{A}$ , a diameter of 2–4 mm (full width at half maximum), and a divergence less than  $0.25^\circ$ . The purity of the  $\text{Ne}^{4+}$  beam from the ECR with respect to metastable states was previously explored by Bannister [16] using electron-impact ionization. A small cross section observed below the expected ground state threshold suggests that only a few percent of the beam is in the metastable state but the statistical uncertainty of the signal in the electron-impact ionization measurements make a reasonable estimate of the metastable fraction impractical.

The  $\text{Ne}^{4+}$  beam is electrostatically merged with the neutral H beam. The ion and atom beams interact along a field-free region of 47 cm, after which the  $H^+$  product ions are magnetically separated from the primary beams and detected by a channel electron multiplier. Since only the  $H^+$  product is measured, the apparatus actually measures electron loss, the sum of electron capture and ionization. However, ionization at these energies is negligible compared to electron capture [17]. The H neutral beam is monitored by measuring secondary emission from a stainless steel plate. The signal rate (hertz) is extracted from backgrounds (kilohertz) by a two-beam modulation technique [13]. An average form factor, which is a measure of the overlap of the two beams, is determined from two-dimensional overlap measurements at three different positions along the merge path. These overlaps are used to determine the merge angle and spread in merge angle between beams needed in the calculation of the relative collision energy for energies less than 1 eV/u (see, e.g., Ref. [11]).

### III. MULTICHANNEL LANDAU-ZENER CALCULATIONS

For the low-energy collisions considered here, molecular-orbital close-coupling calculations are considered to be the most appropriate and accurate theoretical approach. However, the necessary molecular potentials were not available for this system, so the simpler and more schematic MCLZ approach was used. While MCLZ calculations are not always reliable, in systems where the crossings as a function of internuclear separation  $R$  between initial and final states of the electronic potentials are localized and are dominated by radial couplings, the model can provide a good estimate of EC. Specifically for such systems where the MCLZ predictions are borne out by experiment, MCLZ calculations can be used to extend the cross sections to lower energies inaccessible by experiment and to explore isotope effects.

Here, MCLZ calculations were performed following the prescription of Butler and Dalgarno [18], including the H static dipole polarizability in the radial velocity relation, the multichannel probability from the formulation of Janev *et al.* [19], and the low-energy centrifugal-barrier correction of

Chang and Pritchard [20]. Empirical potentials and couplings were determined following Butler and Dalgarno. States of the separated atoms in the initial channel  $\text{Ne}^{4+}(2s^2 2p^2 \ ^3P) + \text{H}(1s \ ^2S)$  correlate with the four molecular states  $^2\Sigma^-$ ,  $^2\Pi$ ,  $^4\Sigma^-$ , and  $^4\Pi$  with approach probability factors of 1/9, 2/9, 2/9, and 4/9, respectively. For the electron-capture channels, all  $LS$  terms were included for  $\text{Ne}^{3+} + \text{H}^+$  which had avoided-crossing distances between  $3a_0$  and  $18a_0$  which included  $\text{Ne}^{3+}$  single-excitation configurations of  $2s^2 2p^2 3s$ ,  $3p$ ,  $3d$ , and  $4s$  and the multiple-excitation terms  $2p^5 \ ^2P^o$  and  $2s 2p^3 3s \ ^4S^o$ . Since rotational couplings were neglected, this resulted in four spin-symmetry MCLZ calculations, one for each of the molecular states above, with 8, 14, 6, and 5 electron-capture channels, respectively. The MCLZ calculations were repeated for the D target.

### IV. RESULTS AND DISCUSSION

Table I lists the measured absolute total EC cross section for  $\text{Ne}^{4+} + \text{H}$  as a function of collision energy. The statistical and total uncertainties are estimated at the 90% confidence level. The total uncertainty corresponds to a quadrature sum of the statistical and systematic errors. For energies less than 1 eV/u, the uncertainty in c.m. collision energy due to the energy spread of the D and  $\text{Ne}^{4+}$  primary beam and the spread in the merge angle (see Ref. [11]) is also shown in the first column of Table I. Figure 1 compares the measured cross sections to the present MCLZ calculations and to previous experiments. While Fig. 1 shows the present measurements to be in agreement with the results of Seim *et al.* [8], there is significant discrepancy with the measurements of Can *et al.* [6] and Huber [7], both of which suggest that the cross section decreases with decreasing energy. All three previous measurements relied on an H target created by dissociation of  $\text{H}_2$ . This technique can lead to normalization problems (e.g., Ref. [4]). Furthermore, the metastable fractions in the ion beams of the previous experiments are unknown.

As can be seen in Fig. 1, the present MCLZ calculations for both the H and D targets show good agreement with our measurements throughout the energy range considered. In particular, for collision energies less than 3 eV/u, the agreement is excellent. The lower-energy measurements, taken with the D target, follow the energy dependence of the D target MCLZ calculations and are consistent with the significant isotope effect predicted for energies less than 5 eV u. The MCLZ calculations reproduce the local peak at  $\sim 50$  eV/u, but the theoretical cross sections are  $\sim 30\%$  smaller. This discrepancy is likely related to the neglect of rotational coupling and short-range nonlocal interactions in the Landau-Zener approximation, both of which become important at the higher energies.

Due to the good agreement between the merged-beam total cross section measurements and the MCLZ calculations, it is reasonable and useful to report the calculated state-selective cross sections for the dominant channels. Figure 2 displays the MCLZ H target state-selective cross sections for capture to the  $2s^2 2p^2 3p$  and  $3d$  configurations of  $\text{Ne}^{3+}$ . Cross sections for capture to the  $3s$ ,  $4s$ ,  $2p^5 \ ^2P^o$ , and  $2s 2p^3 3s \ ^4S^o$  configurations are smaller than  $5 \times 10^{-17} \text{ cm}^2$  for the energy

TABLE I. Ion-atom merged-beams cross section data for  $\text{Ne}^{4+} + \text{H}(\text{D}) \rightarrow \text{Ne}^{3+} + \text{H}^+(\text{D}^+)$  as a function of collision energy. Measurements below (above) 250 eV/u are performed with D (H). See text for details.

| Collision energy (eV/u) | Cross section ( $10^{-16} \text{ cm}^2$ ) | Statistical uncertainty ( $10^{-16} \text{ cm}^2$ ) | Total uncertainty ( $10^{-16} \text{ cm}^2$ ) |
|-------------------------|---|---|---|
| $0.10 \pm 0.02$         | 36.7                                      | 6.6   | 8.0   |
| $0.17 \pm 0.04$         | 23.6                                      | 4.7   | 5.5   |
| $0.31 \pm 0.05$         | 20.2                                      | 6.4   | 6.9   |
| $0.50 \pm 0.04$         | 21.7                                      | 2.3   | 3.5   |
| $0.77 \pm 0.04$         | 16.5                                      | 1.9   | 2.8   |
| 1.11                    | 23.5                                      | 3.7   | 4.6   |
| 1.79                    | 20.2                                      | 2.3   | 3.4   |
| 2.02                    | 19.7                                      | 2.4   | 3.3   |
| 2.69                    | 20.2                                      | 3.2   | 4.0   |
| 3.20                    | 25.6                                      | 2.6   | 4.0   |
| 4.28                    | 26.6                                      | 3.2   | 4.5   |
| 6.50                    | 30.5                                      | 3.4   | 4.9   |
| 10.2                    | 29.8                                      | 1.3   | 3.8   |
| 15.2                    | 35.7                                      | 3.6   | 5.5   |
| 24.2                    | 38.9                                      | 1.8   | 5.0   |
| 32.0                    | 38.0                                      | 2.4   | 5.8   |
| 48.0                    | 44.5                                      | 2.6   | 5.9   |
| 70.4                    | 41.2                                      | 2.5   | 5.6   |
| 104                     | 41.2                                      | 3.3   | 6.0   |
| 145                     | 38.2                                      | 2.3   | 5.2   |
| 195                     | 35.7                                      | 2.9   | 5.2   |
| 286                     | 36.3                                      | 2.2   | 4.8   |
| 371                     | 37.3                                      | 1.9   | 4.8   |
| 403                     | 37.4                                      | 2.6   | 5.2   |
| 471                     | 34.1                                      | 2.1   | 4.5   |
| 548                     | 36.8                                      | 2.2   | 4.9   |
| 621                     | 35.3                                      | 1.4   | 4.4   |
| 857                     | 36.6                                      | 1.5   | 4.6   |
| 1006                    | 38.0                                      | 2.5   | 5.2   |

range considered and therefore not shown. Capture to  $3d$  dominates for the shown collision energies with  $3p$  only becoming significant at the highest energies. The six largest  $LS$  terms from the  $3d$  configuration are also shown in Fig. 2. For collision energies greater than 10 eV/u, the dominant capture channel is the  $2s^2 2p^2(^3P) 3d^4 P$  which peaks near 200 eV/u, accounting for the local maximum in the experimental cross section. For lower energies, the  $3d$  configuration cross section rises due to the increase in the  $2s^2 2p^2(^1D) 3d^2 F$ ,  $^2D$ , and  $^2P$  capture channels. This sharp increase in the cross section is attributed to trajectory effects due to the ion-induced dipole attraction between the reactants. The isotope effect is manifested in the MCLZ calculation purely in the  $3d$  configuration. The ratio between the cross sections with H and D is predicted to be a factor of 1.4 at 0.01 eV/u.

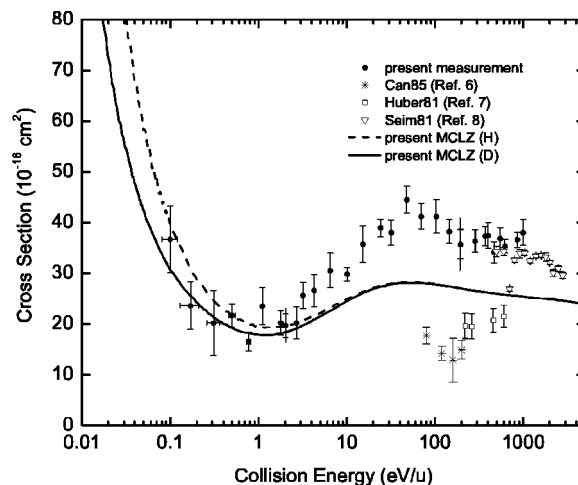


FIG. 1. Ion-atom merged-beam measurements and MCLZ calculations of the electron-capture cross section for  $\text{Ne}^{4+} + \text{H}(\text{D})$  as a function of relative collision energy. Previous experiments are also shown. The statistical errors (estimated at a 90% confidence level) of the present measurements are shown. At energies 2.02 and 195 eV/u both the relative and total errors are shown at a 90% confidence level. For collision energies less than 1 eV/u the uncertainties in center-of-mass collision energy are also shown by horizontal lines. See text for details.

## V. CONCLUSIONS

Using a merged-beams technique, the absolute total electron capture cross section has been measured for  $\text{Ne}^{4+}$  on H (D) for the collision energy range of 0.10–1006 eV/u. The cross section above 250 eV/u was measured with H and below 250 eV/u was measured with D. MCLZ calculations are performed with both H and D from 0.01 to 1000 eV/u and compare well to the measured total cross sections. Below  $\sim 5$  eV/u, the present total cross section calculations show a significant target isotope effect. Agreement between the

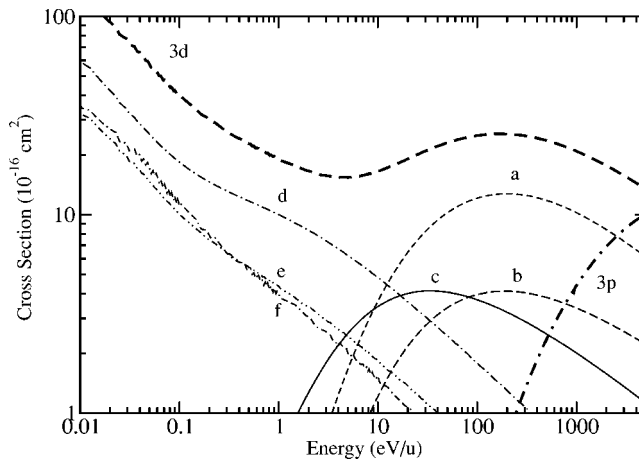


FIG. 2. State-selective MCLZ cross sections for  $\text{Ne}^{4+} + \text{H}$ . Thick lines correspond to capture to the  $\text{Ne}^{3+}$  configurations  $3p$  and  $3d$ . Thin lines correspond to the  $LS$  terms for the  $2s^2 2p^2 3d$  configuration with  $^3P$  core (a)  $^4P$ , (b)  $^2F$ , and (c)  $^2D$ ; and  $^1D$  core (d)  $^2F$ , (e)  $^2D$ , and (f)  $^2P$ .

merged-beam measurements and the MCLZ predicted cross sections gives some confidence in the MCLZ predicted state-selective cross sections.

#### ACKNOWLEDGMENTS

This work was supported by the Division of Chemical Sciences, Office of Basic Energy Sciences and the Division of Applied Plasma Physics, Office of Fusion Energy Sciences, U.S. Department of Energy, Contract No. DE-AC05-

00OR22725 with UT-Batelle, LLC, and by the NASA SARA program under Work Order No. 10,060 with UT-Batelle, LLC. R.R. acknowledges support from the ORNL Postdoctoral Research Associates Program administered jointly by Oak Ridge Institute for Science and Education and Oak Ridge National Laboratory. J.G.W. and P.C.S. acknowledge support from NASA Grant No. NAG5-11453. D.W.S. and M.S. was supported in part by the NASA Space Astrophysics Research & Analysis Grant No. NAG5-5420 and NSF Galactic Astronomy Program Grant No. 0307203.

- 
- [1] G. A. Shield, A. Dalgarno, and A. Sternberg, *Phys. Rev. A* **28**, 2137 (1983).
- [2] S. R. Pottasch and D. A. Beintema, *Astron. Astrophys.* **347**, 975 (1999).
- [3] W. P. West, B. Goldsmith, T. E. Evans, and R. E. Olson, in *Atomic and Molecular Data and Their Applications*, edited by D. R. Schultz, P. S. Krstić, and F. Ownby (AIP, Melville, NY, 2002), p. 171.
- [4] A. Mroczkowski, D. W. Savin, R. Rejoub, P. S. Krstić, and C. C. Havener, *Phys. Rev. A* **68**, 032721 (2003).
- [5] R. Rejoub, M. E. Bannister, C. C. Havener, D. W. Savin, C. J. Verzani, J. G. Wang, and P. C. Stancil, *Phys. Rev. A* **69**, 052704 (2004).
- [6] C. Can, T. J. Gray, S. L. Varghese, J. M. Hall, and L. N. Tunnell, *Phys. Rev. A* **31**, 72 (1985).
- [7] B. A. Huber, *Z. Phys. A* **299**, 307 (1981).
- [8] W. Seim, A. Müller, I. Wirkner-Bott, and E. Salzborn, *J. Phys. B* **14**, 3475 (1981).
- [9] C. C. Havener, F. W. Meyer, and R. A. Phaneuf, in *Physics of Electronic and Atomic Collisions*, edited by W. R. MacGillivray, I. E. McCarthy, and M. C. Standage (AIP, New York, 1992), p. 381.
- [10] C. C. Havener, in *Accelerator-Based Atomic Physics Techniques and Applications*, edited by S. M. Shafroth and J. C. Austin (AIP, Woodbury, NY, 1997), p. 117.
- [11] M. Pieksma, M. Gargaud, R. McCarroll, and C. C. Havener, *Phys. Rev. A* **54**, R13 (1996).
- [12] P. C. Stancil and B. Zygelman, *Phys. Rev. Lett.* **75**, 1495 (1995).
- [13] C. C. Havener, M. S. Huq, H. F. Krause, P. A. Schulz, and R. A. Phaneuf, *Phys. Rev. A* **39**, 1725 (1989).
- [14] C. C. Havener, M. S. Huq, F. W. Meyer, and R. A. Phaneuf, *J. Phys. (Paris), Colloq.* **50**, C1-7 (1989).
- [15] F. W. Meyer, M. E. Bannister, J. W. Hale, C. C. Havener, O. Voitke, and Q. Yan, in *Proceedings of the 13th International Workshop on ECR Ion Sources*, edited by D. P. May and J. E. Ramirez (Texas A&M University Press, College Station, TX, 1997), p. 102.
- [16] M. E. Bannister, *Phys. Rev. A* **54**, 1435 (1996).
- [17] R. K. Janev, L. P. Presnyakov, and V. P. Shevelko, *Physics of Highly Charged Ions* (Springer-Verlag, Berlin, 1985).
- [18] S. E. Butler and A. Dalgarno, *Astrophys. J.* **241**, 838 (1980).
- [19] R. K. Janev, D. S. Belić, and B. H. Brandsen, *Phys. Rev. A* **28**, 1293 (1983).
- [20] A. M. Chang and D. E. Pritchard, *J. Chem. Phys.* **70**, 4524 (1979).